Electronic Supplementary Information

High Symmetric Polyhedral Cu_2O Crystals with Controllable-Index Planes

*Shaodong Sun, Chuncai Kong, Shengchun Yang, Liqun Wang, Xiaoping Song, Bingjun Ding, and Zhimao Yang**

*E-mail: zmyang@mail.xjtu.edu.cn

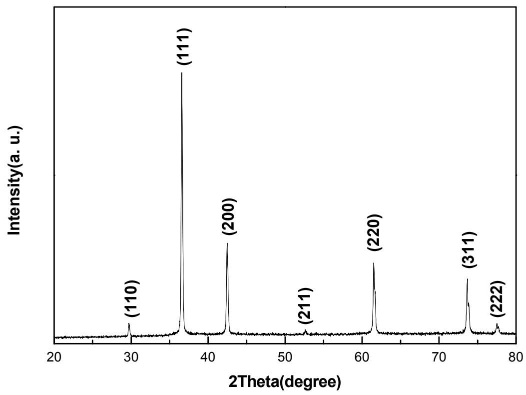

Fig. S1 XRD pattern of the typical as-prepared 50-facet polyhedral Cu_2O crystals.

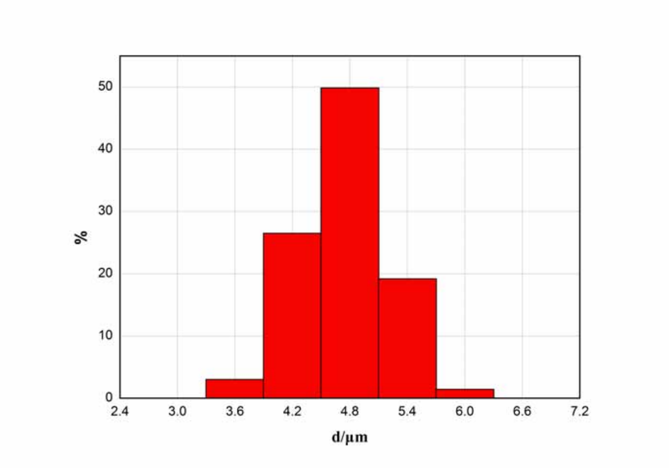

Fig. S2 The size-distribution diagram of as-prepared 50-facet polyhedral Cu_2O crystals.

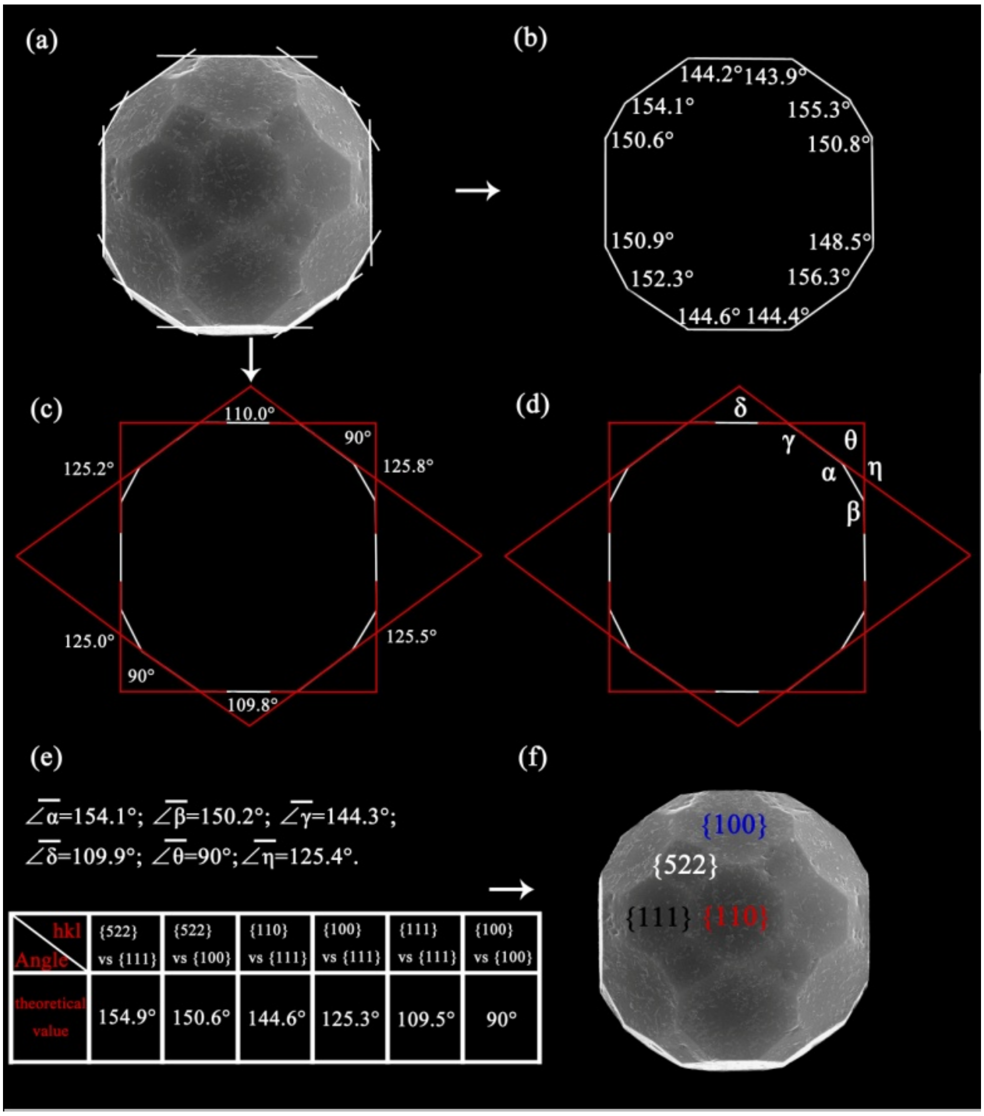

Fig. S3 Determining the facets of 50-facet polyhedral Cu_2O crystals as shown in Fig. 1. (a) SEM image of a 50-facet polyhedral Cu_2O architecture; (b) and (c) interfacial angles of the 50-facet polyhedral Cu_2O crystal; (d) interfacial angles of a 50-facet polyhedral Cu_2O bounded by different facets; (e) calculated and theoretical values of interfacial angles of the 50-facet polyhedral Cu_2O bounded by different facets; (f) corresponding planes of the 50-facet polyhedral Cu_2O bounded by different facets.

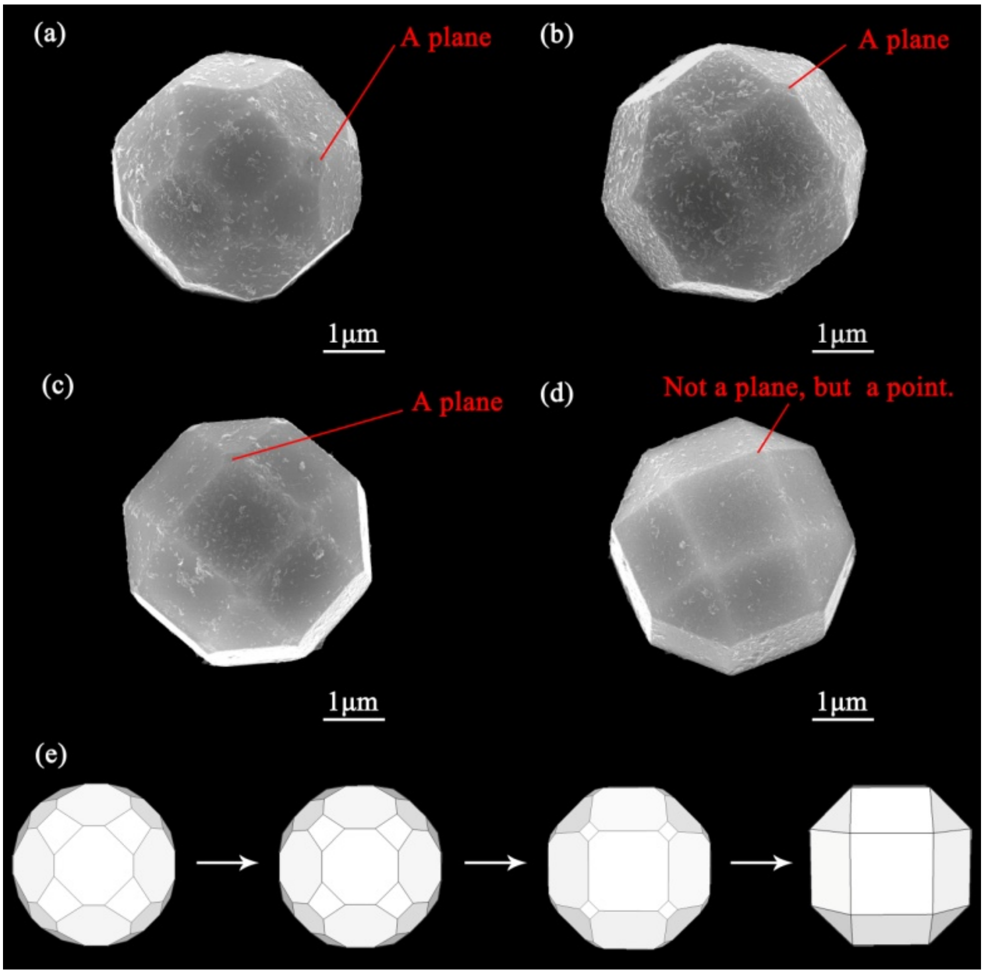

Fig. S4 The enlarged FE-SEM images of the shapes obtained at different reaction time, which can illuminate the shape evolution process from 50-facets to 26-facets polyhedral architectures. (a) 5.5 min; (b) 6.0 min; (c) 7.0 min; (d) 8.0 min; (e) Scheme showing the disappearance process of {522} facets.

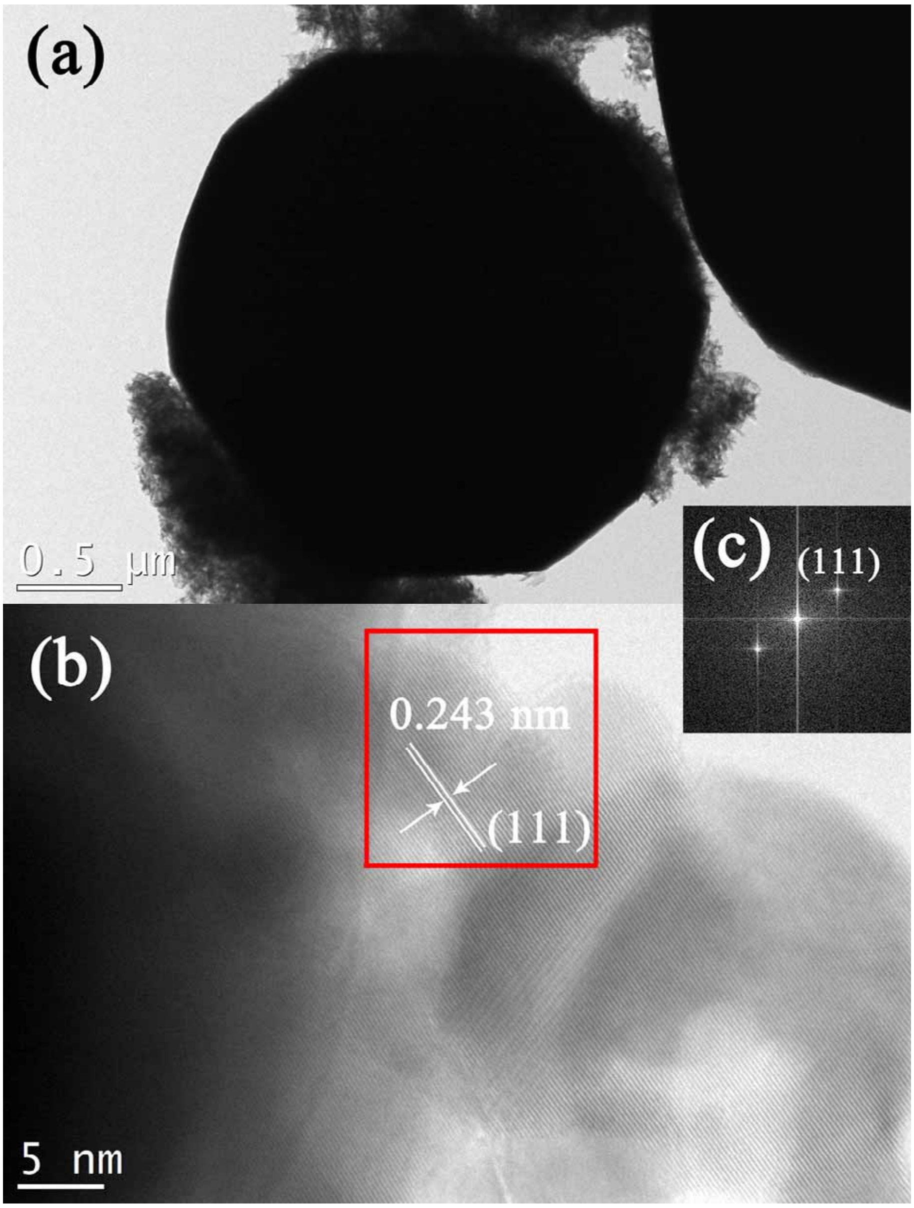

Fig. S5 (a) TEM image of the products obtained at 0.5 min; (b) HRTEM image taken from the area marked with red circle in Fig. S4a; (c) Fourier transform image taken from the areas marked with red squares in Fig. S5b.

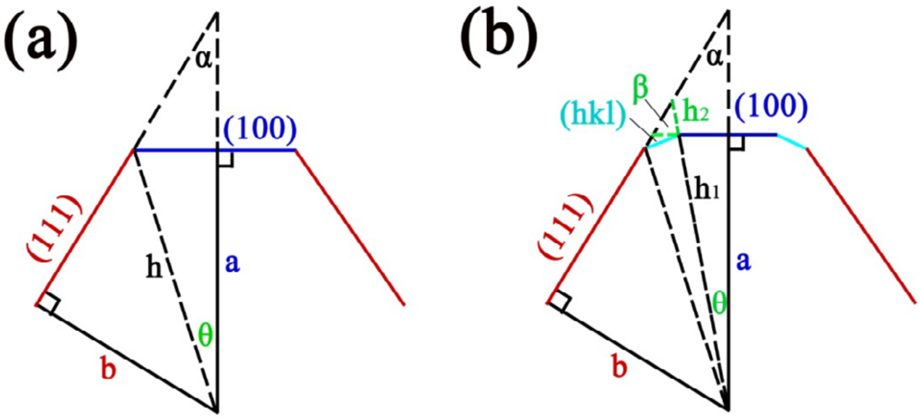

Fig. S6 The relation between R value and morphology of crystal with different index planes. (a) low-index planes; (b) both low-index planes and high-index {hkl} planes.

Detailed calculations of R value and morphology of crystal with different index planes:

(1) As shown in Fig. S6a, the polyhedral architecture is made up of only low-index {100} and {111} facets. The red and blue lines represent the projection of {100} and {111} facets perpendicular to the [110] zone axis, respectively. The theoretical values of angle α = (180°－109.5°) ÷ 2 = 35.25° between {111} vs {111} facets. Where θ is the variable, and R is the function.

∵

$$R = \frac{v_{\{100\}}}{v_{\{111\}}} = \frac{a}{b} = \frac{h\cos\theta}{h\sin(\theta+\alpha)} = \frac{\cos\theta}{\sin(\theta+\alpha)} = \frac{\cos\theta}{\sin(\theta+35.25°)}$$

∴ When θ=0°, R= 1.73, while θ=90°, R= 0.58. It is in good agreement with the previous report by Wang ZL.

Hence, the relation between R values and shapes can be described as the following figure.

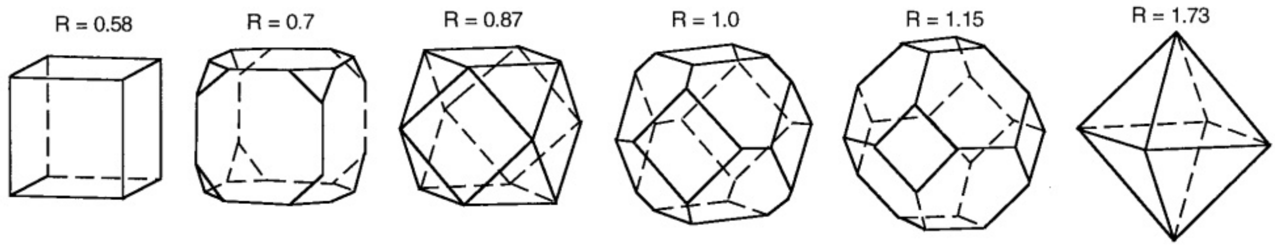

Reference: Wang ZL. Transmission electron microscopy of shape-controlled nanocrystals and their assemblies[J]. Journal of Physical Chemistry B, 2000, 104 (6): 1153-1175.

(2) When the polyhedral architecture is made up of {100}, {111} and high-index {hkl} planes, the projection of {100}, {111} and {hkl} facets perpendicular to the [110] zone axis was shown in Fig. S6b. The red, blue and cyan, lines represent the {111}, {100} and {hkl} planes, respectively. The R value can be calculated based on Fig. S6b, where α = 35.25°, and β = 54.7° is the acute angle between {111} vs {100}. Where θ is the variable, R is the function. Similarly, R value can be described by the following equation.

∵

$$a = h_1 \cos\theta$$

$$b = h_1\left[\frac{\sin(\theta+\alpha) - \cos\theta \cdot \tan\alpha \cdot \sin\beta - \sin\theta \cdot \sin\beta}{1 - \cos\alpha \cdot \sin\beta}\right]$$

$$R = \frac{v_{\{100\}}}{v_{\{111\}}} = \frac{a}{b} = \frac{(1 - \cos\alpha \cdot \sin\beta)\cos\theta}{\sin(\theta+\alpha) - \cos\theta \cdot \tan\alpha \cdot \sin\beta - \sin\theta \cdot \sin\beta}$$

$$\therefore \quad R = \frac{(1 - \cos 35.25° \cdot \sin 54.7°)\cos\theta}{\sin(\theta + 35.25°) - \cos\theta \cdot \tan 35.25° \cdot \sin 54.7° - \sin\theta \cdot \sin 54.7°}$$

Based on the above discussion, it can be seen that the controllable high-index planes can be formed via changing the *R* values under appropriate reaction conditions.

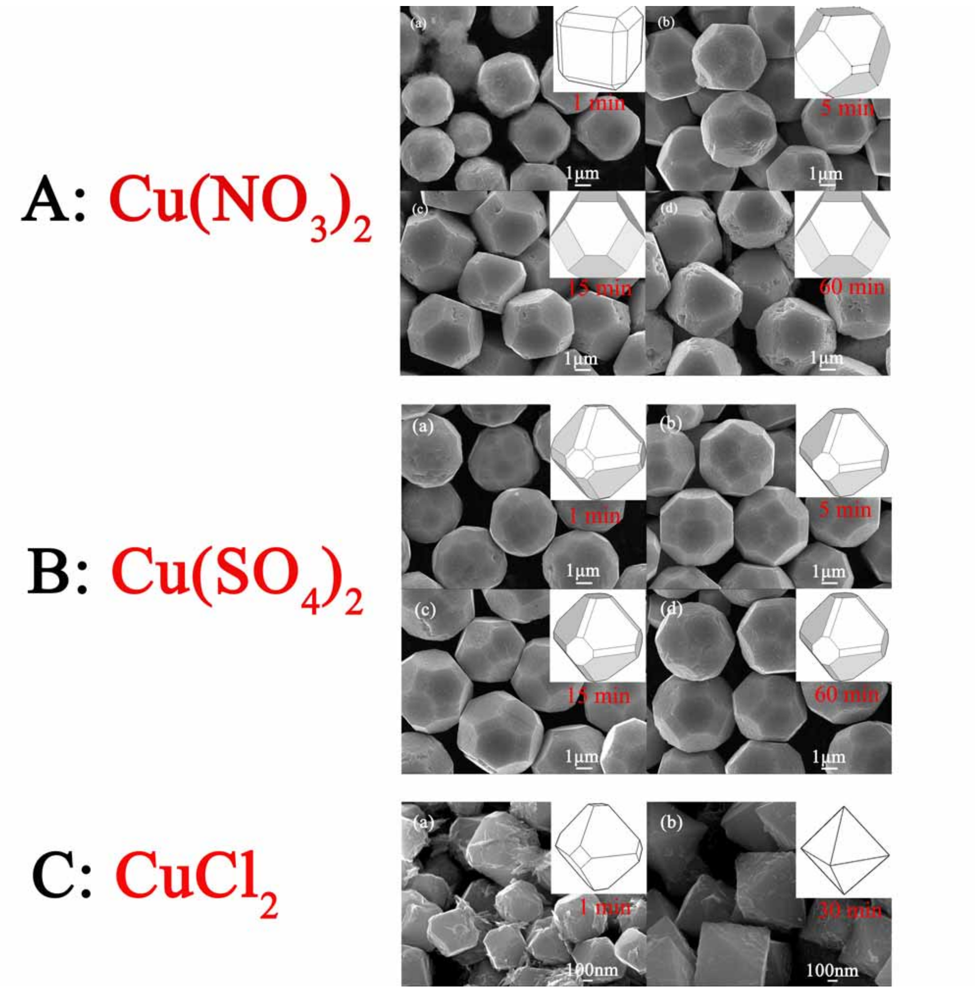

Fig. S7 FESEM images of the products obtained using $Cu(NO_3)_2$, $CuSO_4$ and $CuCl_2$ as copper ions sources under otherwise the same reaction conditions. (A) $Cu(NO_3)_2$; (B) $CuSO_4$; and (C) $CuCl_2$.

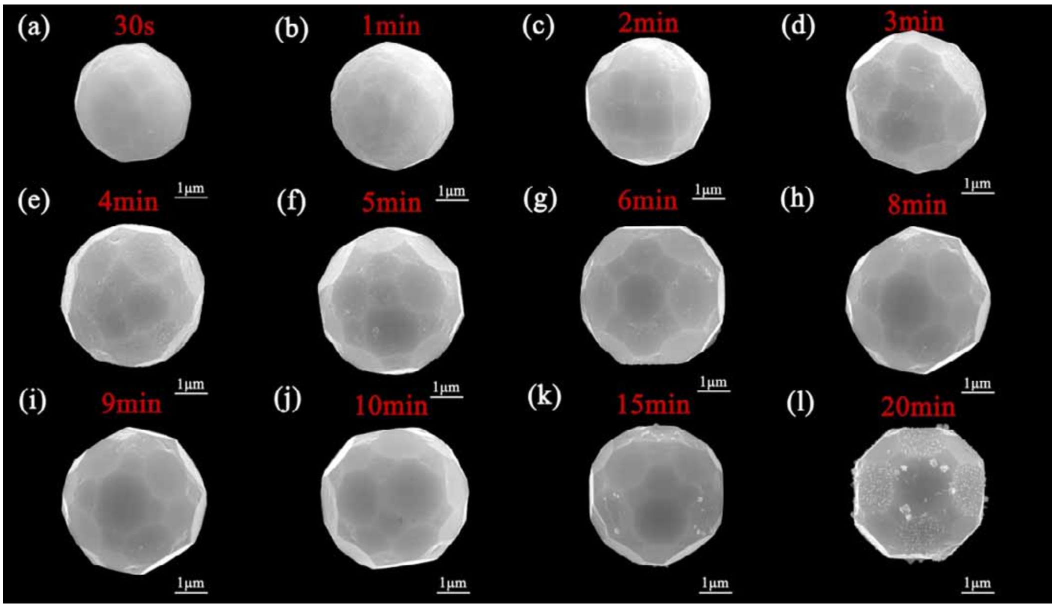

Figure S8. Typical FE-SEM images of the shapes obtained at different reaction time as the amount of D-glucose powder was 0.9 g, (a) 0.5 min; (b) 1 min; (c) 2 min; (d) 3 min; (e) 4 min: (f) 5 min; (g) 6 min; (h) 8 min; (i) 9 min; (j) 10 min; (k) 15 min; (l) 20 min.

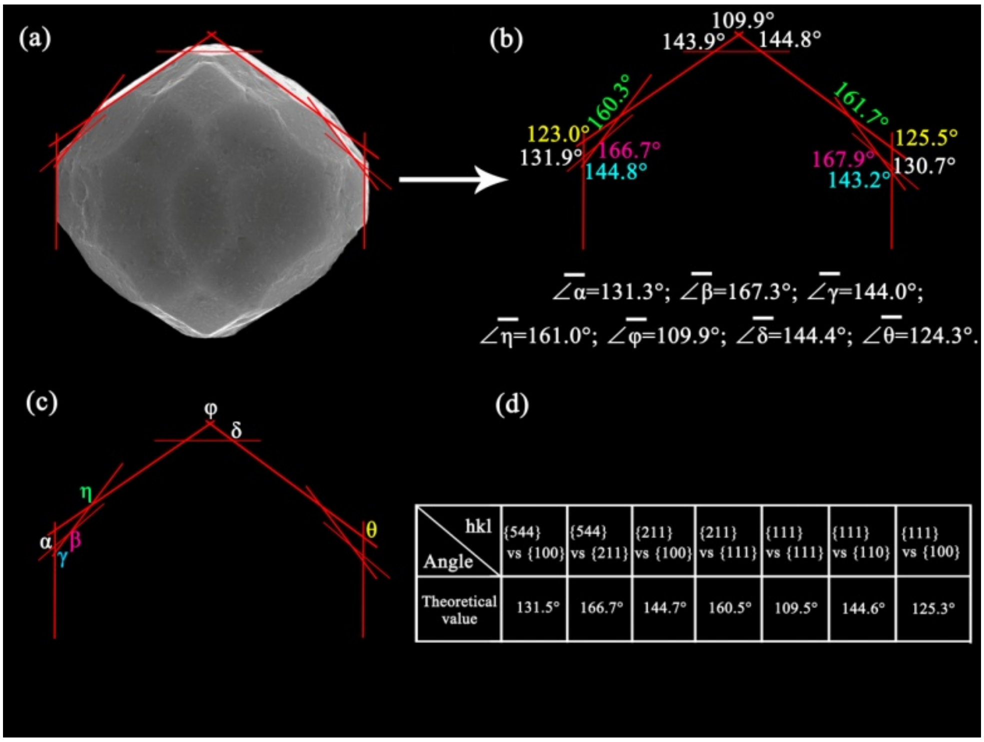

Angle \ hkl	{544} vs {100}	{544} vs {211}	{211} vs {100}	{211} vs {111}	{111} vs {111}	{111} vs {110}	{111} vs {100}
Theoretical value	131.5°	166.7°	144.7°	160.5°	109.5°	144.6°	125.3°

Fig. S9 Determining the facets of 74-facet polyhedral Cu_2O crystals as shown in Fig. 3. (a) SEM image of a 74-facet polyhedral Cu_2O architecture; (b) interfacial angles of the 74-facet polyhedral Cu_2O crystal; (c) interfacial angles of 74-facet polyhedral Cu_2O bounded by different facets; (d) calculated and theoretical values of interfacial angles of 74-facet polyhedral Cu_2O bounded by different facets.

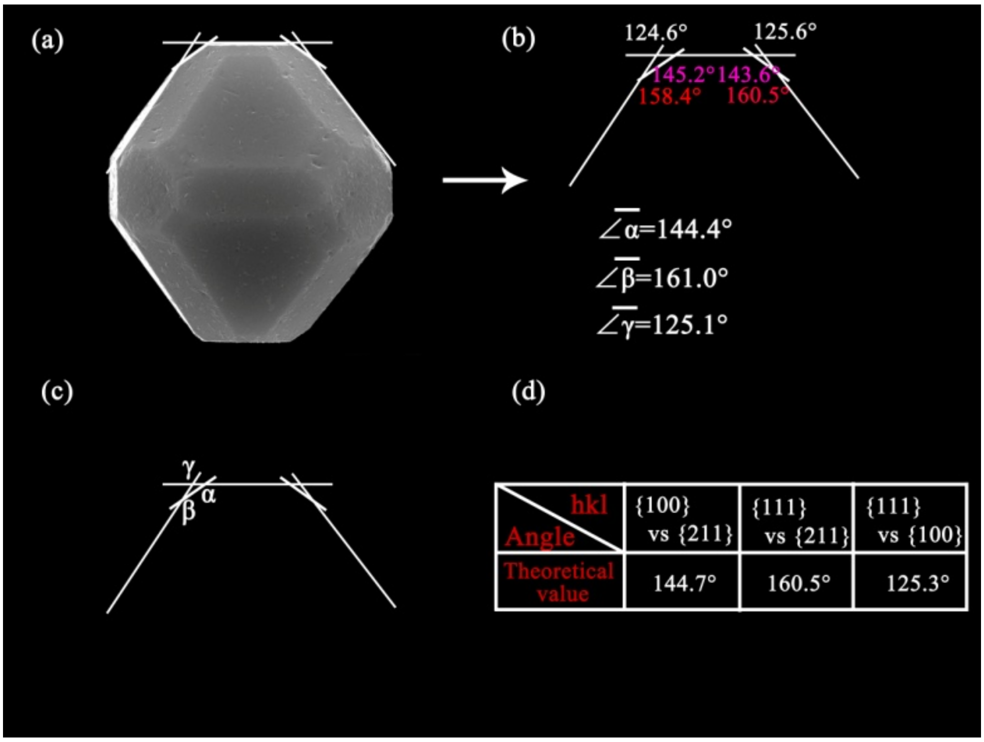

Fig. S10 Determining the facets of 50-facet polyhedral Cu_2O crystals as shown in Fig. 4. (a) SEM image of a 50-facet polyhedral Cu_2O architecture; (b) interfacial angles of the 50-facet polyhedral Cu_2O crystal; (c) interfacial angles of 50-facet polyhedral Cu_2O bounded by different facets; (d) calculated and theoretical values of interfacial angles of 50-facet polyhedral Cu_2O bounded by different facets. Two surface angles of 144.4° and 161.0° are measured (Fig. S10b), which are in good agreement with the theoretical values of angle α = 144.7° and angle β = 161.5 between {211} vs {100} and {211} vs {111}, respectively (Fig. S10d). Moreover, angle of 125.1° was also measured, which is in good agreement with the theoretical values of angle γ = 125.3° between {111} vs {100}. The results suggest that the exposed facets of the 50-facet polyhedral Cu_2O crystal are {211}, {110}, {100} and {111} planes (Fig. 4c).

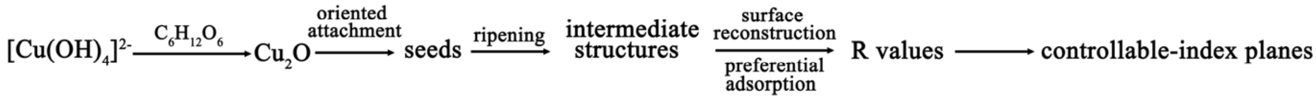

Scheme S1. A schematic illustration of the proposed particle reaction pathways and growth mechanism that lead to the formation of Cu_2O crystals with controllable-index planes. As the essence of our synthesis, the precursor ($[Cu(OH)_4]^{2-}$) is reduced by $C_6H_{12}O_6$ to form Cu_2O atoms, which subsequently aggregate to form nuclei via orient-attachment process. Once these nuclei have grown past a critical size, they will become seeds with varied shapes in different condition. And then seeds will grow into various intermediate structures by ripening process (Fig. 2 and Fig. S7), then these intermediate structures evolved into different polyhedral architectures via surface reconstruction and preferential adsorption in different reaction conditions, which can modify the ratio (R) between the growth rates along the <100> and <111> directions, finally resulting in the shape-controlled synthesis of polyhedral architectures with controllable-index planes.

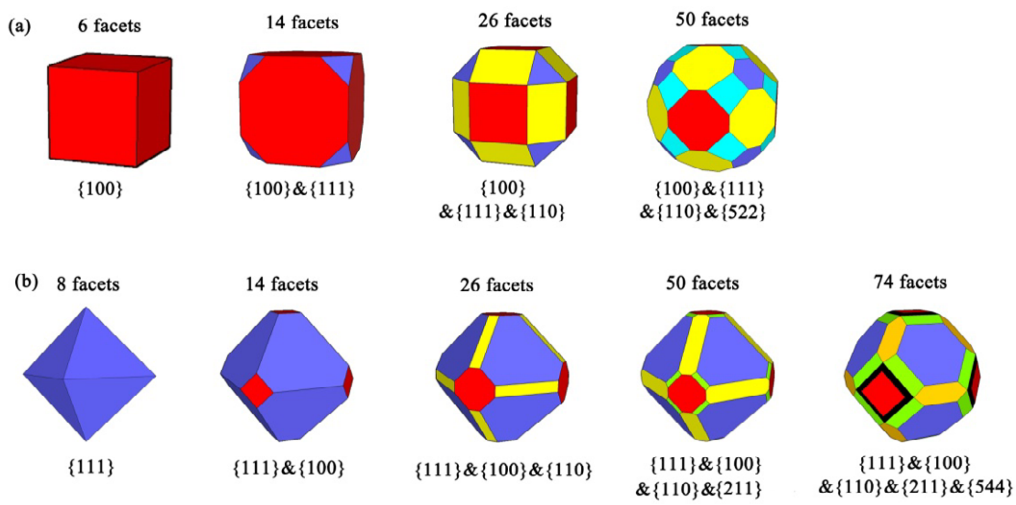

Scheme S2. Geometrical schematic showing the formation of multi-facet polyhedral Cu_2O architectures with high-index planes from cube and octahedron. (a) a shape cutting process of a 50-facet polyhedral Cu_2O architecture with high-index {522} planes from a cube; (b) a shape cutting process of 74-facet and 50-facet polyhedral Cu_2O architecture with high-index {211} and {544} planes from an octahedron. The red, blue, yellow, cyan, green and black colors represent the {100}, {111}, {110}, {522}, {211}, and {544} planes, respectively.

The high-index planes can be designed from a well-defined cube or octahedron, and an interesting schematic model of geometrical shape evolution from cube (6 {100} facets) and octahedron (8 {111} facets) to 50 and 74-facet polyhedral architecture with high-index planes is shown in Scheme S2. From Scheme S2a, it can be seen that a truncated cube with exposed 6 {100} facets (red areas) and 8 {111} facets (blue areas) can be generated from a well-defined cube by “cutting” their 8 corners, and the 12 edges of the truncated cube can be cut to generate 12 rectangular {110} facets (yellow areas), finally a high symmetric 50-facet polyhedron with high-index {522} facets (cyan areas) is formed by further cutting the joints of square, triangular and rectangular facets of a truncated edges cube. This 50-facet polyhedral structure with high-index {522} facets (Fig. 1) can be viewed as a result of cutting a cube. Similarly, another 50-facets polyhedral architecture (Fig. 4) with high-index {211} facets (green areas) can be fabricated via cutting an octahedron (Scheme S2b), and 74-facets polyhedral architecture (Fig. 3) with high-index {544} facets (black areas) is also formed by further cutting the edges between {100} (red areas) and {211} facets (green areas) of this 50-facets polyhedron. Herein, facile and high-yield fabrication of high symmetric multi-facet polyhedral Cu_2O crystals enclosed by low-index {111}, {100} and {110} facets, and controllable high-index facets (including {522}, {211}, and {544} facets) as shown in the above mentioned geometrical schematic illustration were successfully synthesized by a template-free complex precursor solution route.